International Journal of Engineering Trends and Technology
ISSN: 2231 – 5381 / https://doi.org/10.14445/22315381/IJETT-V71I3P202

Volume 71 Issue 3, 9-16, March 2023

Original Article

Thermography Study on Distribution Transformer in Substation: Transformer Core Material

Mardzulliana Zulkifli[1], Muhammad Zulqarnain Muthaza[2], Iqbal Safaat[2], Sim Sy Yi[2], and Norain Sahari[2]

[1]*Fakulti Kejuruteraan Elektronik dan Kejuruteraan Komputer, Universiti Teknikal Malaysia Melaka, Durian Tunggal, Melaka, Malaysia*
[2]*Faculty of Engineering Technology, Universiti Tun Hussein Onn Malaysia, Campus Pagoh, Muar, Johor, Malaysia*

[1]*Corresponding Author : zulliana@uthm.edu.my*

Received: 26 September 2022 Revised: 12 January 2023 Accepted: 17 March 2023 Published: 25 March 2023

Abstract *- Switchgear and terminations for transmission and distribution lines are all parts of an electrical system known as a transformer substation. Transformer substations can possibly even better convert voltage from high to low. Especially for distribution networks, the thermal performance of power substations is a significant concern. The heat generated by a transformer's operation raises the temperature of its internal components. Transformers with higher efficiency rise in temperature less quickly than those with lower efficiency. Heat damage that occurs to the transformer windings during normal operation is one of the main causes of damage. SolidWorks' thermal simulation software, thermal method analysis, was utilised to assess thermal performance. In this project, amorphous metal and amorphous steel are employed as the two material cores to compare and simulate the thermal analysis in rising temperature and heat flux. When compared to actual tests, which had restrictions on the thermal result, the simulation's results can be used to help choose the right material. The maximum temperature the simulation determines between amorphous metal and amorphous steel is 60 ℃. The heat flux result indicates an initial value of 6 x 10^4 W/m2 and an increase in the metal's thermal conductivity to 60 ℃. As a result, amorphous metal was suggested as a potential for transformer core material.*

Keywords *- Deep learning, Heat, Temperature, Thermal image, Transformer core, Thermography.*

1. Introduction

The current flowing through an electrical component generates heat in power substation equipment like current transformers (CT), potential transformers (PT), insulators, breakers, arresters, and disconnectors. The infrared thermal radiation patterns, communicated as heat energy in the target barriers, are invisible to the human eye. The exterior heat pattern of any component can only be seen by heat-based infrared imaging devices [1].

Infrared imaging technology can be highly useful in locating defects in high-voltage electrical devices in their early stages before a major breakdown occurs. Power substation components have a longer working and safe lifecycle when an image-based diagnosis is utilised. Any electrical equipment with a temperature exceeding 0°C emits thermal radiation, which can cause the interior temperature of high-voltage electrical equipment to increase.

To obtain the thermal characteristics of high-voltage electrical components, infrared thermal imaging (IRT) employs sophisticated infrared (IR) cameras. The infrared image still shows the electrical components' temperature profile and temperature range. In electrical apparatus, various temperature ranges are represented by various colour schemes. The heat profile, which rates the rank of the defective components by the issues regarding maintenance of the components, can be used by thermographs to understand the infrared picture models. The inspection of the heated components and their repair in accordance with the electrical equipment's order is the final outcome of this [2].

In steady-state models, the hotspot temperature and its position are predicted along with the temperature field in the transformer winding. A technique called thermal 3D modeling simulation is used to precisely forecast temperature increases in components and windings above ambient temperature. Determining the hotspot position and temperature increases is crucial for industry and transformer users. Thermal cameras are used to collect genuine data to compare with. Due to the ability to detect thermal performance, calibration for thermal cameras is a problem. The project's goal is to create a 3D modeling simulation and incorporate a thermal camera that is more effective to utilize, given that it is used in industry.

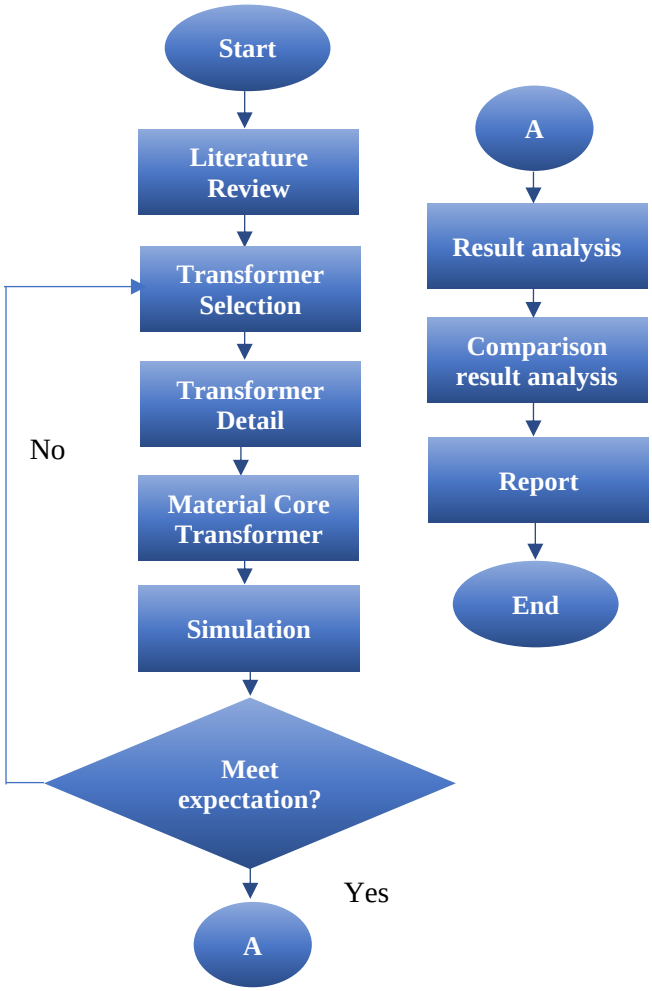

Fig. 1 Project Flowchart

Infrared thermal imaging (IRT) uses potent infrared (IR) cameras to gather the thermal properties of high-voltage electrical components. The infrared image still shows the electrical components' phase profile and temperature range. Different colour schemes in electrical equipment are used to indicate different temperature ranges. Thermographs may analyse infrared picture models by using the heat profile, which ranks the rank of the defective components by the serious measures of maintenance of the components. The inspection of the heated components and their repair in accordance with the electrical equipment's order is the final outcome of this [2].

Due to its non-intrusive, quick, and cost-effective methodology, the IR imaging strategy is currently a key technology for anticipating and preventing the flaws of multiple substances in various areas. A survey of the literature indicates that, as a result, the infrared imaging methodology offers several applications and practical methods for the operational functioning of electrical equipment without interfering with the system's operation [2-14].

In order to increase reliability, thermal method analysis is necessary. To assess the reliability of power transformers, simulation software is employed. However, this approach lacks details on the modes and operating circumstances of power transformers as well as the definition of test sample items. The heating process and magnetic flux between two material cores—amorphous steel and metal—are compared in this work using simulation.

2. Method

A simulation has been created to facilitate this research's objectives and make the procedure more accurate. This was the start of linking research to studies from earlier investigations. The benefit of finishing this research results from this strategy. The recommended approach to finish the research investigation was indicated in the previous study. This research continues because of the suggestions that are suggested for addition. After that, SolidWorks software was used to create the 3D modelling. This core transformer's 3D modelling dimension was derived from an earlier research hypothesis. The transformer for this study has the same dimension.

Additionally, this latest copy sure the project stayed within its parameters and fulfilled its goal. The flowchart shown in Figure 1 illustrates the project's overall process flow.

The selection of transformers was chosen based on the similarity of power used by Tenaga Nasional Berhad (TNB) at the distribution substation. Figure 2 shows the transformer selection; a site visit to the industry at Malaysia Marine and Heavy Engineering (MMHE) on 14 April 2022 was used to discover a transformer suited for this study. As a result of the site visit, a transformer in Figure 2, the 66kV/470V transformer, was selected for this study.

Fig. 2 Transformer 66 kV, 470 V at MMHE.

Table 1. Parameter for amorphous steel

Parameter	Specification
kVA rating	3500
Voltage rating	6600/470 V
Maximum magnetic flux	1.1 Wb/m
Window space factor (kW)	0.273
Stacking factor	0.9

Table 2. Parameter for amorphous metal

Parameter	Specification
kVA rating	3500
Voltage rating	6600/470 V
Maximum magnetic flux	1.2 Wb/m
Window space factor (kW)	0.273
Stacking factor	0.9

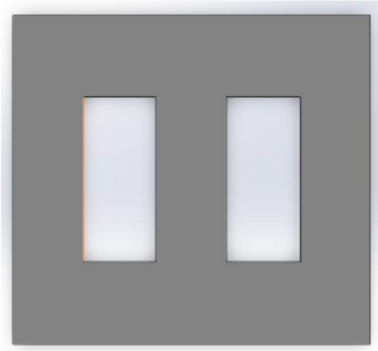

Fig. 3 Transformer core

The design of a three-phase transformer rating 3500 kVA 6600/470 V using parameters obtained from a site visit is shown in Table 1 and Table 2 for material, amorphous steel and amorphous metal.

Figure 3 shows a drawing made with the SolidWorks 3D modelling programme details the transformer core's architecture. The overall dimension of the chosen concept must be established before commencing the detailed design, as doing so will make sketching the detailed design simpler in the future. SolidWorks streamlines the design process and has the ability to turn 2D drawings into 3D models—core transformers' specific technical specifications, which are only available from the manufacturer.

The designed transformer is simulated using Solidworks 3D modelling. Each part is given a set of material properties after the model has been imported. Amorphous metal and amorphous steel will be the main materials in this simulation. In order to assign material qualities, some factors are used similarly to the manufacturing parameters. The model was meshed and simulated using thermal analysis. In order to achieve more precise results using the combined volume of three-phase transformers, fine meshing is needed, as shown by the mesh 3D modelling in Figure 4.

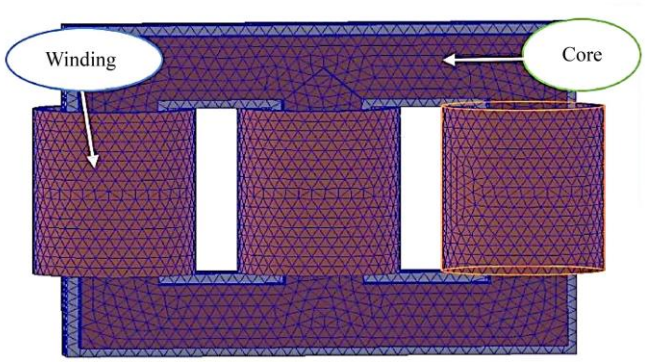

Fig. 4 Mesh 3D modelling

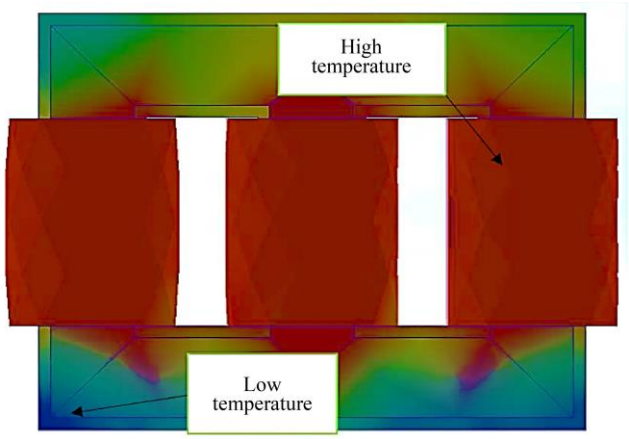

Fig. 5 Simulation Finite Element Analysis (FEA)

Figure 5 illustrates how the material is heated during a simulated thermal investigation. As a result of the heat and infrared radiation being emitted, the various colours depict how hot it is. For instance, red denotes a high temperature, whereas blue denotes a low temperature.

Amorphous steel and amorphous metal will be contrasted as two cores. Typically, these materials are utilised to create transformer cores. Amorphous metals are non-crystalline or glassy and are also referred to as vitreous metals. From these metals, high-performance transformers are created. The materials' low conductivity aids in reducing eddy currents.

Next are amorphous steel cores, which reduce eddy current flow by using multiple paper-thin metallic strips. Amorphous steel cores act at greater temperatures than conventional lamination layers and charge fewer losses than other magnetic cores. It is required to compare and assess the design efficiency with the existing and proposed designs after the design simulation using SolidWorks methods, where these two materials' attributes were applied. The temperature and heat flux between the two materials can be compared after the comparison.

Transformer specification data received and used as a reference in the simulation were provided via a site visit to MMHE, as shown in Table 3.

Table 3. Specification of transformer

Parameter	Specification
Rated power (kVA)	3500
High / Low Voltage	6600/470 V
Phase	3
Frequency	60 Hz
Winding temperature rise ℃	60/65

3. Result and Discussion

This section primarily deals with analysing and discussing obtained results and comparisons from outcome simulation in connection to the project objectives. In this project, two materials were simulated using Solidworks to produce a thermal analysis that outputs temperature and heat flux.

On a three-phase, 3500kVA, 6600/440 V system, the simulation is conducted. The total number of nodes and produced elements and the element size and tolerance are all included in Table 4 mesh data.

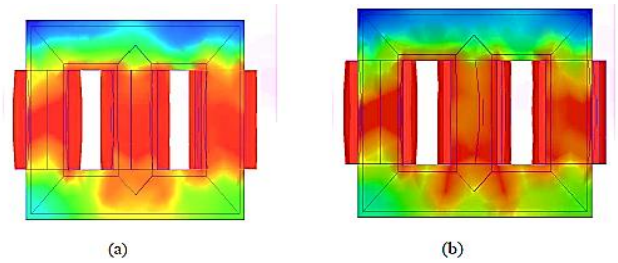

Fig. 6 Temperature of amorphous metal (a) t = 10s, (b) t = 20s

Table 4. Mesh data

No. of node	Number of elements	Element size (mm)
1339	3761	70.502

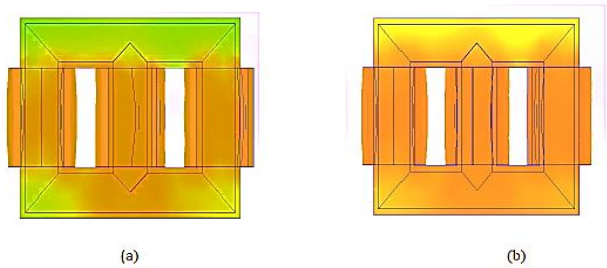

Fig. 7 Temperature of amorphous steel (a) t = 10s, (b) t = 20s

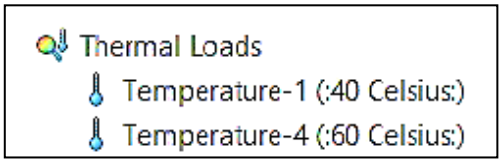

Fig. 8 Parameter of ambient temperature

Amorphous metal and amorphous steel are two core materials that are compared in Figure 9 using temperature versus time graphs(s). According to the graph, the amorphous steel reacts more quickly than the amorphous metal to a change in temperature over the course of one second when the steel is 45°C, and the metal is 35°C. When temperatures rise, metal materials can react more quickly than steel materials. This is because amorphous steel, a soft magnetic material, is employed in electrical power transformers, motors, and generators.

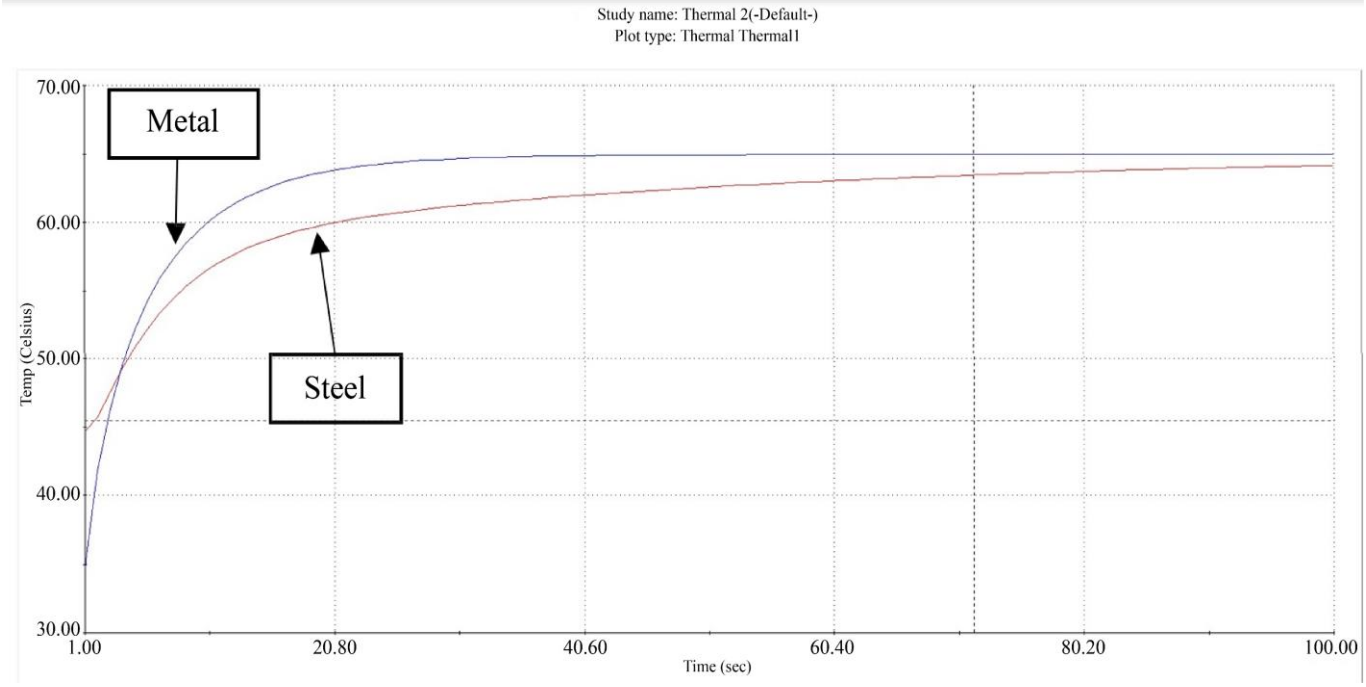

Fig. 9 Temperature rise between amorphous metal and steel

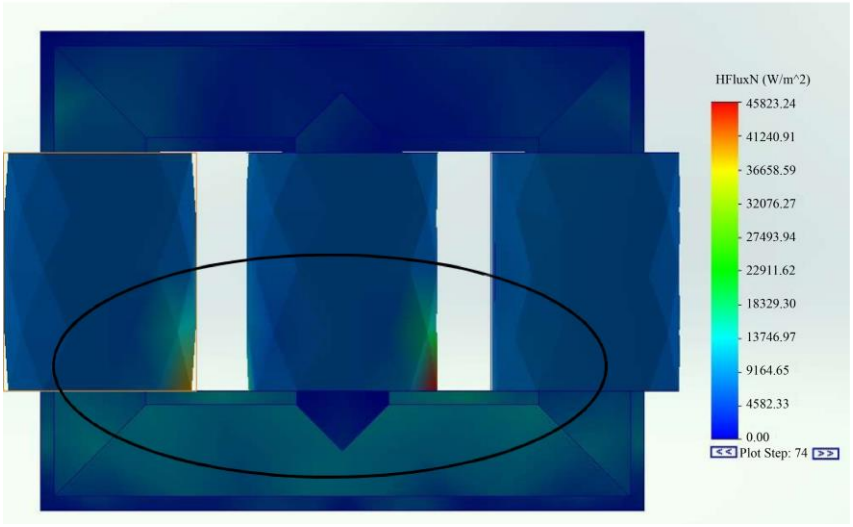

Fig. 10 Heat flux for Amorphous Metal

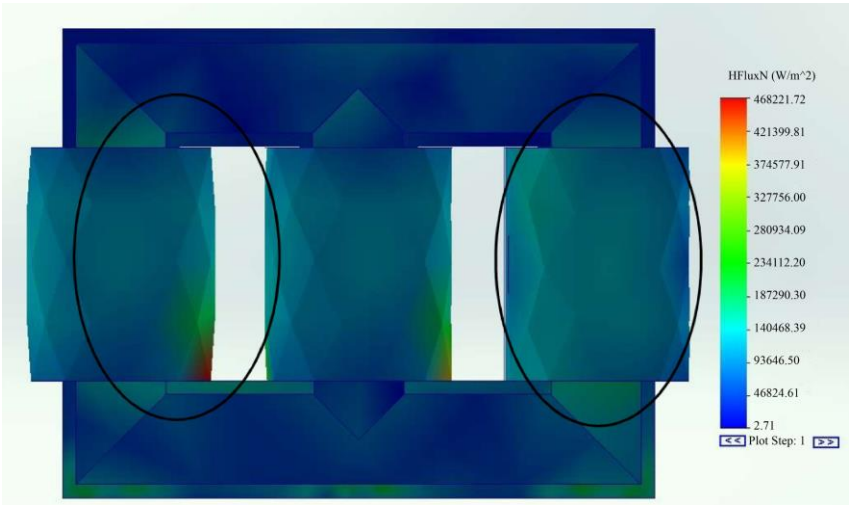

Fig. 11 Heat flux for Amorphous steel

Amorphous steel cores are more responsive at greater temperatures than other magnetic cores and offer reduced losses. Although these amorphous metals have a lesser response when the transformer is in use, they are used to create high-performance transformers. The graph also demonstrates that steel starts to heat up around 45 degrees but reacts more slowly than metal, which starts to heat up at 35 degrees. The metal, however, reacts quickly and reaches 60 °C in 10 s as opposed to 20 s for steel.

Figures 10 and 11 compare the heat flux between steel and metal through heat flux models. Figure 10 shows that the amorphous metal substance's surface only differs at the winding region, which has a different colour. Additionally, the red patch's centre and left limb core portions are encircled in winding. The heat flow in the simulated amorphous steel material is different from the heat flux in amorphous metal, in any case. The surface area colour change is more obvious in the Figure 11 simulation results than in Figure 10.

As a result, it can be said that amorphous metal is superior to amorphous steel because the heat on the surface heats up more slowly than heat flowing to the surface.

Understanding how it changes shape and how it compares to other materials is vital because the heat transfer at the metal–steel interface is a measure that directly influences the surface's final structure. The heat transfer coefficient in the metal and steel interface was calculated using the simulated temperature in the metal and steel, which mimics the change in heat flux.

As shown in Figure 12, after a substantial initial variation, the heat transfer coefficient in the metal interface under heat flow gradually decreases over time to a value of approximately $6x10^4$ W/m^2, which is stabilized by the gap air that forms as a result of the metal's contraction. Steel, in contrast, has a small drop until it reaches 2×10^4 W/m^2.

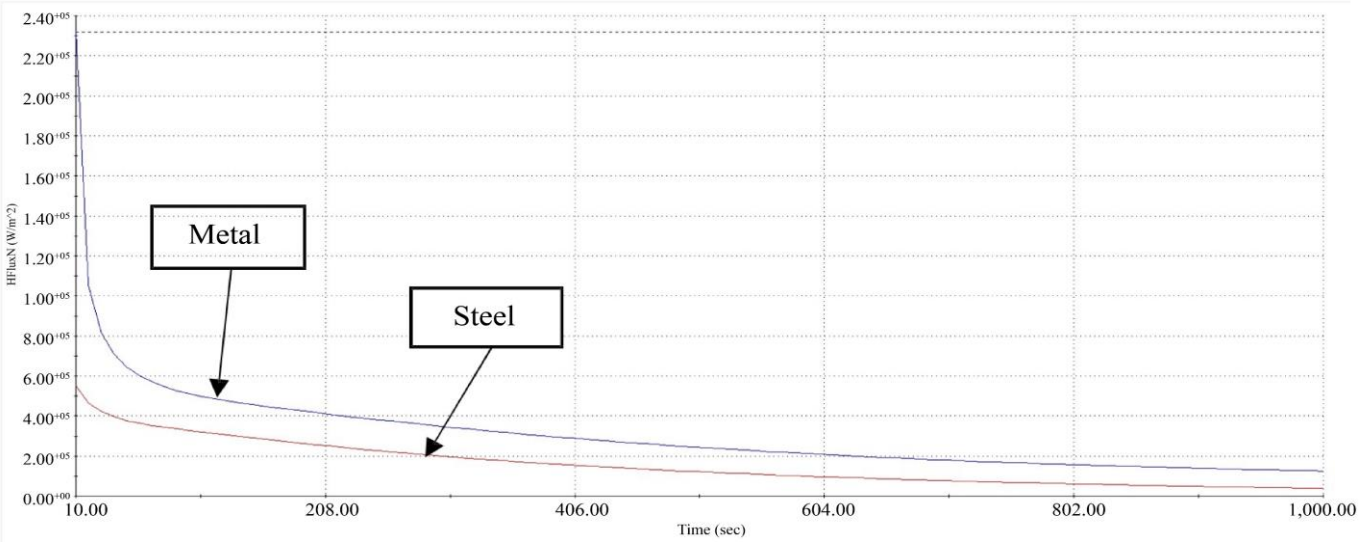

Fig. 12 Heat flux density between amorphous metal and steel

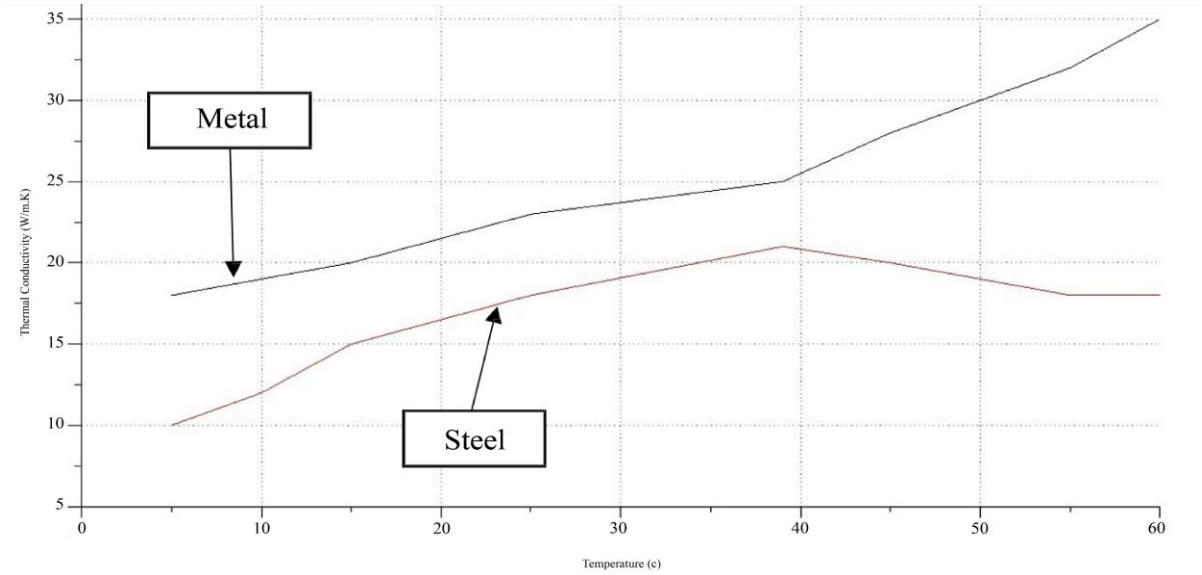

Fig. 13 Thermal conductivity between amorphous steel and metal

Table 5. Comparison of amorphous metal and steel

Core material / Testing	Amorphous metal	Amorphous steel
Temperature rise	Fast reaction	Slow reaction
Heat flux	Slow on heat transfer	High transfer heat to the surface
Thermal conductivity	High conductivity	Low conductivity

Thermal conductivity, a property of materials, describes the capacity to conduct heat. Figure 13 illustrates how the metal's thermal conductivity increased as the temperature rose up to 40°C and then rose to 60°C.

Amorphous steel's thermal conductivity improved with temperatures up to 21°C before significantly declining at higher temperatures. According to the graph, amorphous steel has one of the lowest heat conductivity values of any metal. In contrast to amorphous metal, materials with high thermal conductivity could move heat more quickly and effectively than those with low conductivity.

Table 5 provides a summary of the results for choosing an appropriate core material for three-phase transformers based on the three types of testing carried out on the two types of core materials.

4. Conclusion

Solidworks simulations were used to assess the heat flow in the scenario of a surface core between amorphous steel and amorphous metal. The graph was used to compare the temperature increase and heat flux transfer between the two materials. While the simulation was running, the simulation graph was obtained. Two cores are contrasted in terms of temperature rise and heat flux. In addition to showing that metal is more suitable than steel at different temperatures and times, the heat flow graph shows that metal is more stable. Steel is less effective than metal in terms of thermal conductivity.

Acknowledgments

As the PhD students at Universiti Teknikal Malaysia Melaka, the authors would like to thank the Universiti Tun Hussein Onn Malaysia for supporting this research under the Tier 1 Grant Scheme (Code H931).

References

[1] Z. Korendo, and M. Florkowski, "Thermography-Based Diagnostics of Power Equipment," *Power Engineering Journal*, vol. 15, no. 1, pp. 33-42, 2001. [CrossRef] [GoogleScholar] [Publisher Link]

[2] Zhihua Ge et al., "Performance Monitoring of Direct Air-Cooled Power Generating Unit with Infrared Thermography," *Applied Thermal Engineering*, vol. 31, no. 4, pp. 418-424, 2011. [CrossRef] [GoogleScholar] [Publisher Link]

[3] B.B. Lahiri et al., "Medical Applications of Infrared Thermography: A Review," *Infrared Physic Technology*, vol. 55, no. 4, pp. 221-235, 2012. [CrossRef] [GoogleScholar] [Publisher Link]

[4] Paul Gill, *Electrical Power Equipment Maintenance and Testing*, CRC Press: Boca Raton, FL, USA.

[5] C Bougriou, "Measurement of the Temperature Distribution on a Circular Plane Fin by Infrared Thermography Technique," *Applied Thermal Engineering*, vol. 24, no. 5-6, pp. 813-825, 2004. [CrossRef] [GoogleScholar] [Publisher Link]

[6] C.A. Balaras, and A.A. Argiriou, "Infrared Thermography for Building Diagnostics," *Energy and Buildings*, vol. 34, no. 2, pp. 171-183, 2002.[CrossRef] [GoogleScholar] [Publisher Link]

[7] Royo, R., et al., "Thermographic Study of the Preheating Plugs in Diesel Engines," *Applied Thermal Engineering*, vol. 37, pp. 412-419, 2012. [CrossRef] [GoogleScholar] [Publisher Link]

[8] M. Manana, "Field Winding Fault Diagnosis in DC Motors During Manufacturing Using Thermal Monitoring," *Applied Thermal Engineering*, vol. 31, no. 5, pp. 978-983, 2011.[CrossRef] [GoogleScholar] [Publisher Link]

[9] D. J. Titman, "Applications of Thermography in Non-Destructive Testing of Structures," NDT E International, vol. 34, no. 2, pp. 149154, 2001. [GoogleScholar] [Publisher Link]

[10] A. Rahman Al-Kassir, "Thermographic Study of Energetic Installation," *Applied Thermal Engineering*, vol. 25, no. 2-3, pp. 183-190, 2005. [CrossRef] [GoogleScholar] [Publisher Link]

[11] Mohd Shawal Jadin, and Soib Taib, "Recent Progress in Diagnosing the Reliability of Electrical Equipment by Using Infrared Thermography," *Infrared Physics & Technology*, vol. 55, no. 4, pp. 236-245, 2012. [CrossRef] [GoogleScholar] [Publisher Link]

[12] Improving Electrical System Reliability with Infrared Thermography Source, 2019. [Online]. Available: http://www.infraredelectrical.com/index.html

[13] Diptak Pal et al, "Real-Time Condition Monitoring of Substation Equipment Using Thermal Cameras," *IET Generation, Transmission & Distribution*, vol. 12, no. 4, pp. 895-902, 2018. [CrossRef] [GoogleScholar] [Publisher Link]

[14] Qasim Khan, Asfar A. Khan, and Furkan Ahmad, "Condition Monitoring Tool for Electrical Equipment—Thermography," *2016 International Conference on Electrical, Electronics, and Optimization Techniques*, pp. 2802-2806, 2016. [CrossRef] [GoogleScholar] [Publisher Link]

[15] B. Durai Babu et al., "Transformer Health Monitoring System Using GSM Technology," *SSRG International Journal of Electronics and Communication Engineering*, vol. 9, no. 11, pp. 11-16, 2022. [CrossRef] [Publisher Link]

[16] Priscilla Whitin, and V. Jayasankar, "A Novel Deep Learning-Based System for Real-Time Temperature Monitoring of Bone Hyperthermia," *SSRG International Journal of Electrical and Electronics Engineering*, vol. 10, no. 1, pp. 187-196, 2023. [CrossRef] [Publisher Link]

[17] P.Sundar, and A.Santhi, "Thermal Energy Storage in Building Using Phase Change Materials(PCMS)," *SSRG International Journal of Thermal Engineering*, vol. 1, no. 2, pp. 27-32, 2015. [CrossRef] [Publisher Link]

[18] D. Sheema et al., "An Algorithm for Detection and Identification of Infestation Density of Pest-Fall Armyworm in Maize Plants Using Deep Learning Based on Iot, " *International Journal of Engineering Trends and Technology*, vol. 70, no. 9, pp. 240-251, 2022. [CrossRef] [GoogleScholar] [Publisher Link]

[19] S.L.Meena, "Spectral and Thermal Properties of Ho3+ Doped Aluminum- Barium- Calcium-Magnesium Fluoride Glasses," *SSRG International Journal of Applied Physics*, vol. 7, no. 1, pp. 14-20, 2020. [CrossRef] [Publisher Link]

[20] Pal Durgeshkumar K, and Sudhakar Umale, "Numerical Investigation on Air Side Performance of Fin and Tube Heat Exchnagers with Different Types of Fins," *SSRG International Journal of Thermal Engineering*, vol. 1, no. 2, pp. 1-6, 2015. [CrossRef] [GoogleScholar] [Publisher Link]

[21] Vivek Kumar, and S. R. Shah, "Thermobiological Mathematical Model for the Study of Temperature Response After Cooling Effects," *SSRG International Journal of Applied Physics*, vol. 9, no. 2, pp. 7-11, 2022. [CrossRef] [Publisher Link]

[22] Biloa Otiti Sandrine Olive et al., "Physico-Chemical and Thermal Characterisation of Canarium Schweinfurthii Engl (Cs) Shells," *SSRG International Journal of Material Science and Engineering*, vol. 7, no. 3, pp. 9-15, 2021. [CrossRef] [Publisher Link]